

# The competition of C-X $\cdots$ O=P halogen bond and $\pi$ -hole $\cdots$ O=P bond between halopentafluorobenzenes C<sub>6</sub>F<sub>5</sub>X (X=F, Cl, Br, I) and triethylphosphine oxide

Xiao Ran Zhao · Hui Wang · Wei Jun Jin

Received: 9 August 2013 / Accepted: 8 September 2013 / Published online: 26 September 2013  
© Springer-Verlag Berlin Heidelberg 2013

**Abstract** Calculation predicted the interacting forms of halopentafluorobenzene C<sub>6</sub>F<sub>5</sub>X (X=F, Cl, Br, I) with triethylphosphine oxide which is biologically interested and easily detected by <sup>31</sup>P NMR. The interaction energy and geometric parameters of resultant halogen or  $\pi$ -hole bonding complexes were estimated and compared. Moreover, the bonding constants were determined by <sup>31</sup>P NMR. Both theory and experiments indicated the C<sub>6</sub>F<sub>6</sub> and C<sub>6</sub>F<sub>5</sub>Cl interact with triethylphosphine oxide by  $\pi$ -hole bonding pattern, while C<sub>6</sub>F<sub>5</sub>I by halogen/ $\sigma$ -hole bonding form. For C<sub>6</sub>F<sub>5</sub>Br, two interactions are comparative and should coexist competitively. The calculated interaction energies of  $\sigma$ -hole bonding complexes,  $-5.07$  kcal mol<sup>-1</sup> for C<sub>6</sub>F<sub>5</sub>Br $\cdots$ O=P and  $-8.25$  kcal mol<sup>-1</sup> for C<sub>6</sub>F<sub>5</sub>I $\cdots$ O=P, and  $\pi$ -hole bonding complexes,  $-7.29$  kcal mol<sup>-1</sup> for C<sub>6</sub>F<sub>6</sub> $\cdots$ O=P and  $-7.24$  kcal mol<sup>-1</sup> for C<sub>6</sub>F<sub>5</sub>Cl $\cdots$ O=P, are consistent with the changing tendency of bonding constants measured by <sup>31</sup>P NMR, 4.37, 19.7, 2.42 and 2.23 M<sup>-1</sup>, respectively.

**Keywords** Calculation · Competition · Halogen bond ·  $\pi$ -hole bond · <sup>31</sup>P NMR ·  $\sigma$ -hole bond · Halopentafluorobenzene · Triethylphosphine oxide

## Introduction

During recent decades, various new intermolecular specific interaction forces have been paid attention besides conventional van der Waals force and hydrogen bond. Halogen bond or named  $\sigma$ -hole bond is the typical example of those new noncovalent and directional interaction forces and has become

a hot topic in recent decades [1–8]. The weak interactions involving aromatic  $\pi$ -systems include  $\pi$ - $\pi$  stacking [9–16], cation-/anion- $\pi$  interaction [17–21], and so on, which exist widely in biological fields and their importance appears increasingly in materials science and molecular recognition. The investigation shows the ions usually tend to interact with the center of benzene ring by electrostatic force in cation- $\pi$  and anion- $\pi$  models [22, 23]. It is noteworthy that changing the substituents on the aromatic rings should make the interaction pattern relative to  $\pi$ -system dramatically changed, e.g., from cation- $\pi$  interaction to anion- $\pi$  interaction [21]. Fluorine atoms as one of the classical strong electron-withdrawing groups could decrease the  $\pi$ -electron density of the substituted benzene. The positive electrostatic potential region on both sides perpendicular to aromatic ring plane of halopentafluorobenzenes appears, named as  $\pi$ -hole [24], which resembles closely the term  $\pi$ -hole proposed by Politzer et al. [25–27] in inorganic and nonconjugated molecules, while the positive electrostatic potential region on halogen atom along the expanding direction of C-X axial, named as  $\sigma$ -hole [7, 8, 25–27]. Both  $\sigma$ -hole and  $\pi$ -hole [24] appear simultaneously as fluorine congeners with larger radius, chlorine, bromine and iodine atoms bind to benzene rings. The electrostatic attraction interaction between the  $\sigma$ -hole or  $\pi$ -hole [24] and electron-rich group/site is defined as  $\sigma$ -hole bond/halogen bond [7, 8, 25–29] or  $\pi$ -hole bond [24]. Importantly,  $\sigma$ -hole bond can also involve groups IV–VI besides halogens [26, 28]. In the case of halopentafluorobenzenes, both  $\sigma$ -hole and  $\pi$ -hole bonds with negative site are possible and they should be competitive or cooperative. Ma [30] and Zhang et al. [31] studied the interactions between the halopentafluorobenzenes and solvents by <sup>13</sup>C NMR combining with computational chemistry. They noticed that changing trends of <sup>13</sup>C NMR chemical shift of chloro- and bromopentafluorobenzenes with Lewis basic solvent (C<sub>6</sub>D<sub>6</sub>, etc.) were similar with that of perfluorobenzene (moving to higher frequency, or lower field), which was different from iodopentafluorobenzenes (moving to lower frequency, or higher

X. R. Zhao · H. Wang · W. J. Jin (✉)  
College of Chemistry, Beijing Normal University, Beijing 100875,  
The People's Republic of China  
e-mail: wjjin@bnu.edu.cn

field). So, they concluded by combining calculation that halogen bonding occurs between iodopentafluorobenzenes and solvent molecules, while  $\pi$ -hole bonding occurs between other halopentafluorobenzenes or perfluorobenzene and solvent molecules. The competition or cooperation between halogen bond and  $\pi$ -hole bond should be significant in materials engineering or molecular recognition.

At present, the interaction of halopentafluorobenzenes with triethylphosphine oxide is studied by calculation and  $^{31}\text{P}$  NMR spectroscopy in inert solvent. Triethylphosphine oxide as  $\sigma$ -hole or  $\pi$ -hole bonding acceptor may be significant in biological fields due to the possible intermolecular interaction participated by O=P group, and also the easy detection of  $^{31}\text{P}$  NMR. It is expected to explore the relationship between  $\sigma$ -hole/halogen bond and  $\pi$ -hole bond using triethylphosphine oxide as acceptor. Based on the calculation of geometric parameters, interaction energy, cooperative energy of the bonding complexes combining with  $^{31}\text{P}$  NMR spectroscopy, the conclusion is reached that  $\pi$ -hole bond is dominant in hexafluorobenzene and chloropentafluorobenzene,  $\sigma$ -hole bond is dominant in iodopentafluorobenzene,  $\sigma$ -hole and  $\pi$ -hole bond interactions may coexist for bromopentafluorobenzene.

## Computational and experimental details

### Computational

All calculations were carried out with GAUSSIAN 09 quantum chemistry package in the electronic ground state using  $\omega$ B97XD/AUG-CC-PVDZ of dispersion-corrected density functional theory (DFT-D) [32–34] with the 6-311++G\*\* basis set for H, C, F, P, O, Cl, Br atoms and pseudopotential basis set LANL2DZdp for I atom (<https://bse.pnl.gov/bse/portal>).

The steered molecular dynamic (SMD) model was used to simulate solvation effect of n-hexane [35]. All molecules were optimized in energy and structure.

The interaction energy ( $\Delta E$ ) of  $\sigma$ -hole or  $\pi$ -hole complexes was obtained as the difference between the energy of the optimized complex and the sum of the total energies of the optimized monomers:  $\Delta E = E_{\text{AB}} - (E_{\text{A}} + E_{\text{B}})$ . The trimers were treated as dimers to calculate interaction energy, that is, the energy of  $\sigma$ -hole bonding in trimer was obtained as the difference between the energy of trimer and the sum of the total energies of trimethylphosphine oxide and  $\pi$ -hole bonding complex. Similarly, the energy of  $\pi$ -hole bonding in trimer was obtained as the difference between the energy of trimer and the sum of the total energies of trimethylphosphine oxide and  $\sigma$ -hole bonding complex. The cooperative energy ( $\Delta E_{\text{coop}}$ ) was the energy change of  $\sigma$ -hole or  $\pi$ -hole bond due to the introduction of  $\pi$ -hole or  $\sigma$ -hole bond, which was obtained as the difference between the sum of energies of  $\sigma$ -hole and  $\pi$ -hole bonding in dimer and in trimers. Triethylphosphine oxide was

replaced by trimethylphosphine oxide in order to reduce the cost of computation.

### Reagents and instruments

Triethylphosphine oxide, 97 %, was purchased from Sigma-Aldrich Co. (Shanghai). Diphenylphosphinyl chloride, 98 %, was purchased from Alfa Aesar Co. (WardHill, MA, USA). The extra-dried n-hexane, 98 %, was purchased from Acros Organic Co. Perfluorobenzene, 99 %, was purchased from Alfa Aesar Co. (WardHill, MA, USA). Chloropentafluorobenzene, 99 %, was purchased from Matrix Scientific Co. Bromopentafluorobenzene and iodopentafluorobenzene, all 99 %, were purchased from ABCR Co. (Karlsruhe, Germany). All other non-extra-dried reagents were treated by calcined 3 Å molecular sieves.

$^{31}\text{P}$ -NMR spectra were collected on a Bruker Avance III (Bruker Corporation) 400 MHz spectrometer under static and 2.5 mm magic-angle spinning (MAS) conditions at 298 K. The preparation of all samples was performed in a glove box under nitrogen atmosphere. The sample and external standard  $(\text{C}_6\text{H}_5)_2\text{POCl}$  were added to the external and inner tubes, consisting of a 5 mm coaxial NMR tube. The proton decoupling method was used during the measurement to ensure accuracy and sensitivity; the measurements used a scanning number of 32 and an experimental temperature of 25 °C. All experiments were repeated twice.

### The determination of binding constants by $^{31}\text{P}$ NMR

The n-hexane solution of 0.1 mol L<sup>-1</sup> triethylphosphine oxide was prepared. Different amount of halopentafluorobenzene was directly dissolved in 0.1 mol L<sup>-1</sup> triethylphosphine oxide solution to obtain a series of mixed solution with certain molar ratio, from 0 to over the stoichiometry.

Changes in the chemical shifts of  $^{31}\text{P}$ -NMR were employed to determine the binding constant  $K_{\text{a}}$  by Hughes's method [36], given the  $\sigma$ -hole/ $\pi$ -hole bond donor form 1:1 complex with acceptor.

$$\Delta\delta = (\delta_{\text{max}} - \delta_0) ([\text{C}]/[\text{D}]_0) \quad (1)$$

where  $\Delta\delta$  is the observed change in chemical shift, ( $\Delta\delta$ ),  $\delta_{\text{max}}$  refers to the maximum change of chemical shift as the formation of  $\sigma$ -hole/ $\pi$ -hole bonding complex,  $\delta_0$  represents the chemical shift of 0.1 mol L<sup>-1</sup> O=PET<sub>3</sub> monomer in n-hexane,  $[\text{D}]_0$  equals to O=PET<sub>3</sub> concentration, 0.1 mol L<sup>-1</sup> and  $[\text{C}]$  is determined as solution of the quadratic (2):

$$[\text{C}]^2 + (-[\text{D}]_0 - [\text{A}]_0 - 1/K_{\text{a}})[\text{C}] + [\text{D}]_0[\text{A}]_0 = 0 \quad (2)$$

where  $[\text{A}]_0$  refers to halopentafluorobenzene concentration,  $K_{\text{a}}$  is binding constant. Nonlinear curve-fitting of the experimental  $\Delta\delta$  vs  $[\text{A}]_0$  to the expression (2), from experiments at

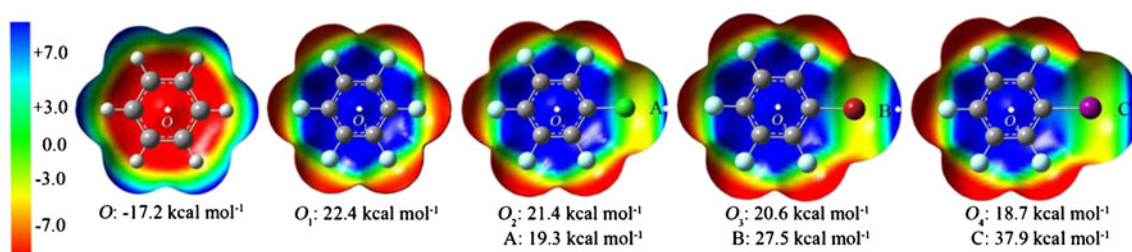


**Fig. 1** Electrostatic potential surface of halopentafluorobenzenes computed at  $\omega$ B97X-D/6-311++G\*/LANL2DZdp level

known  $[D]_0$  and  $[A]_0$ , yielded parameters  $\delta_{\max}$ ,  $[C]$  and  $K_a$ . Curve-fitting was repeated 2–3 times, using different sets of initial guess values,  $\delta_{\max}$ ,  $[C]$  and  $K_a$ , for these parameters, yielding stable values in all cases.

## Results and discussion

### The molecular surface electrostatic potentials

Haloperfluorobenzenes are one kind of excellent halogen bonding donors, for example, 1,2- or 1,4-diiodotetrafluorobenzene has been used widely in crystal engineering [24, 37–40]. Figure 1 shows the calculated electrostatic potential surface of benzene and several haloperfluorobenzenes. Due to strong electron-withdrawing substituent, fluorine, Cl, Br and I on benzene ring display a positive electrostatic potential region, i.e.,  $\sigma$ -hole [7, 8, 25–27, 41], in halopentafluorobenzenes. Moreover, the negative electrostatic potential region ( $\rho$ :  $-17.2$  kcal mol $^{-1}$ )

on both sides of benzene becomes the positive one as F is the full substituent due to the reduction of electron charge density, i.e.,  $\pi$ -hole [24].

In perfluorobenzene or all halopentafluorobenzenes, there is no  $\sigma$ -hole on F atom, thus F can not act as a donor to participate in halogen bond. However, the area and the maximum value ( $V_{s,\max}$ ) of positive surface electrostatic potential region on halogen atom increases gradually from Cl, Br to I atom as the increase of atomic number, atomic radii and polarizability. As shown in Fig. 1, the  $V_{s,\max}$  is  $19.3$  kcal mol $^{-1}$  in  $C_6F_5Cl$ ,  $27.5$  kcal mol $^{-1}$  in  $C_6F_5Br$  and  $37.9$  kcal mol $^{-1}$  in  $C_6F_5I$ . On the other hand,  $\pi$ -hole has the  $V_{s,\max}$  at the center,  $22.4$  kcal mol $^{-1}$  for  $C_6F_6$ ,  $21.4$  kcal mol $^{-1}$  for  $C_6F_5Cl$ ,  $20.6$  kcal mol $^{-1}$  for  $C_6F_5Br$  and  $18.7$  kcal mol $^{-1}$  for  $C_6F_5I$ , respectively. The decrement order of the maximum surface electrostatic potential of  $\pi$ -hole obeys the reversed order of electron-withdrawing ability of halogen atoms.

It can be seen from the calculated electrostatic potential that perfluorobenzene has solely  $\pi$ -hole, so it forms  $\pi$ -hole

**Fig. 2** Fully optimized structures of  $\sigma$ -hole and  $\pi$ -hole bonding dimer and trimer complexes between halopentafluorobenzenes and trimethylphosphine oxide simulated at  $\omega$ B97X-D/6-311++G\*/LANL2DZdp level

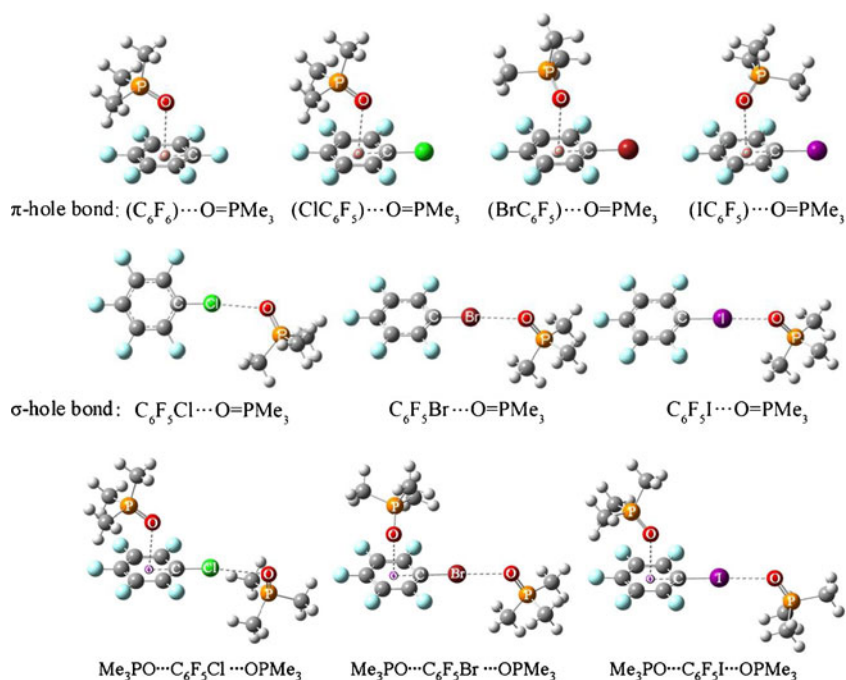


**Table 1** Key geometric parameters of dimer and trimer complexes of  $\sigma$ -hole and  $\pi$ -hole bonds

Parameters		$\pi$ -hole bonding complexes				$\sigma$ -hole bonding complexes		
		C <sub>6</sub> F <sub>6</sub>	C <sub>6</sub> F <sub>5</sub> Cl	C <sub>6</sub> F <sub>5</sub> Br	C <sub>6</sub> F <sub>5</sub> I	C <sub>6</sub> F <sub>5</sub> Cl	C <sub>6</sub> F <sub>5</sub> Br	C <sub>6</sub> F <sub>5</sub> I
$d_{o/X\cdots O}/\text{\AA}$	dimer	2.906	2.927	2.932	2.957	2.836	2.792	2.755
	trimer		2.928	2.966	2.986	2.847	2.824	2.798
$\angle C-o/C-X\cdots O/^\circ$	dimer	84.8	85.0	88.3	93.7	174.3	178.0	178.7
	trimer		86.1	93.8	88.3	166.1	178.5	178.7
$\angle P=O\cdots o/X/^\circ$	dimer	123.4	120.3	119.6	123.5	122.6	128.8	130.4
	trimer		123.1	125.1	128.0	104.2	126.3	124.7

bond with acceptor. Other halopentafluorobenzenes have both  $\pi$ - and  $\sigma$ -holes. The  $V_{s,max}$  (19.3 kcal mol<sup>-1</sup>) of  $\sigma$ -hole for chloropentafluorobenzene is less than that of  $\pi$ -hole (21.4 kcal mol<sup>-1</sup>), so it can be expected that it forms mainly  $\pi$ -hole bond with acceptor. While the  $V_{s,max}$  of  $\sigma$ -hole for bromopentafluorobenzene or iodopentafluorobenzene is greater than that of  $\pi$ -hole, the two should form the  $\sigma$ -hole/halogen bond with acceptor predominantly or competitively.

#### Geometric parameters of halogen bonding and $\pi$ -hole bonding complexes

The possibility of forming the halogen bonding and  $\pi$ -hole bonding complexes has been predicted by surface electrostatic potential of halopentafluorobenzenes. In the following part, the possible complexes using triethylphosphine oxide as acceptor are optimized in geometric structure and interaction energy.

Figure 2 shows the optimized structures of the complexes of halopentafluorobenzenes and trimethylphosphine oxide, and their geometric parameters are listed in Table 1. It can be seen from Fig. 2 that oxygen atom in trimethylphosphine oxide can interact with the center of  $\pi$ -hole on benzene ring to form  $\pi$ -hole bond complex, which is consistent with the maximum position of surface electrostatic potential at the center of benzene ring of halopentafluorobenzene. Table 1 shows the distance from oxygen atom to the  $\pi$ -hole center-*o* is *ca.* 2.9 Å, 13.9 % shorter than 3.37 Å, the sum of their van der Waals radii (O 1.52 Å and the half of ring thickness 1.85 Å). As halogen atomic radius becomes greater and electron-negativity becomes smaller, the surface electrostatic potential at center-*o* becomes smaller, while the distance from oxygen atom to the  $\pi$ -hole center-*o* becomes longer, indicating the strength of  $\pi$ -hole bond weaker. In addition, the oxygen atom stands almost perpendicularly above the center-*o* with very small tilt due to steric effect of triethylphosphine oxide. The angle  $\angle P=O-o$  is *ca.* 120° which is dependent on the orbital direction of lone electron pairs of oxygen atom with respect to aromatic plane.

As stated above, any fluorine atom in C<sub>6</sub>F<sub>6</sub> has no possibility to form  $\sigma$ -hole bond (halogen bond) due to no  $\sigma$ -hole on

fluorine atom. However, as polarizability of halogen atoms become stronger from chlorine to iodine, the ability to produce  $\sigma$ -hole becomes stronger leading to sequent stronger  $\sigma$ -hole bond (halogen bond). Figure 2 shows geometric structures of the halogen bonding complexes between halopentafluorobenzenes and trimethylphosphine oxide. Table 1 indicates that the bond length of Cl $\cdots$ O, Br $\cdots$ O and I $\cdots$ O in dimers is 2.836 Å, 2.792 Å and 2.755 Å, respectively. They are 13.3 %, 17.2 % and 21.3 % shorter than the sum of van der Waals radii of relative interacting atoms. In terms of the change tendency of bond length, the halogen bond becomes stronger from chloropentafluorobenzene, bromopentafluorobenzene to iodopentafluorobenzene. In addition, halogen bond appears to have good linear directionality,  $\angle C-Cl\cdots O=174.3^\circ$ ,  $\angle C-Br\cdots O=178.0^\circ$  and  $\angle C-I\cdots O=178.7^\circ$ .

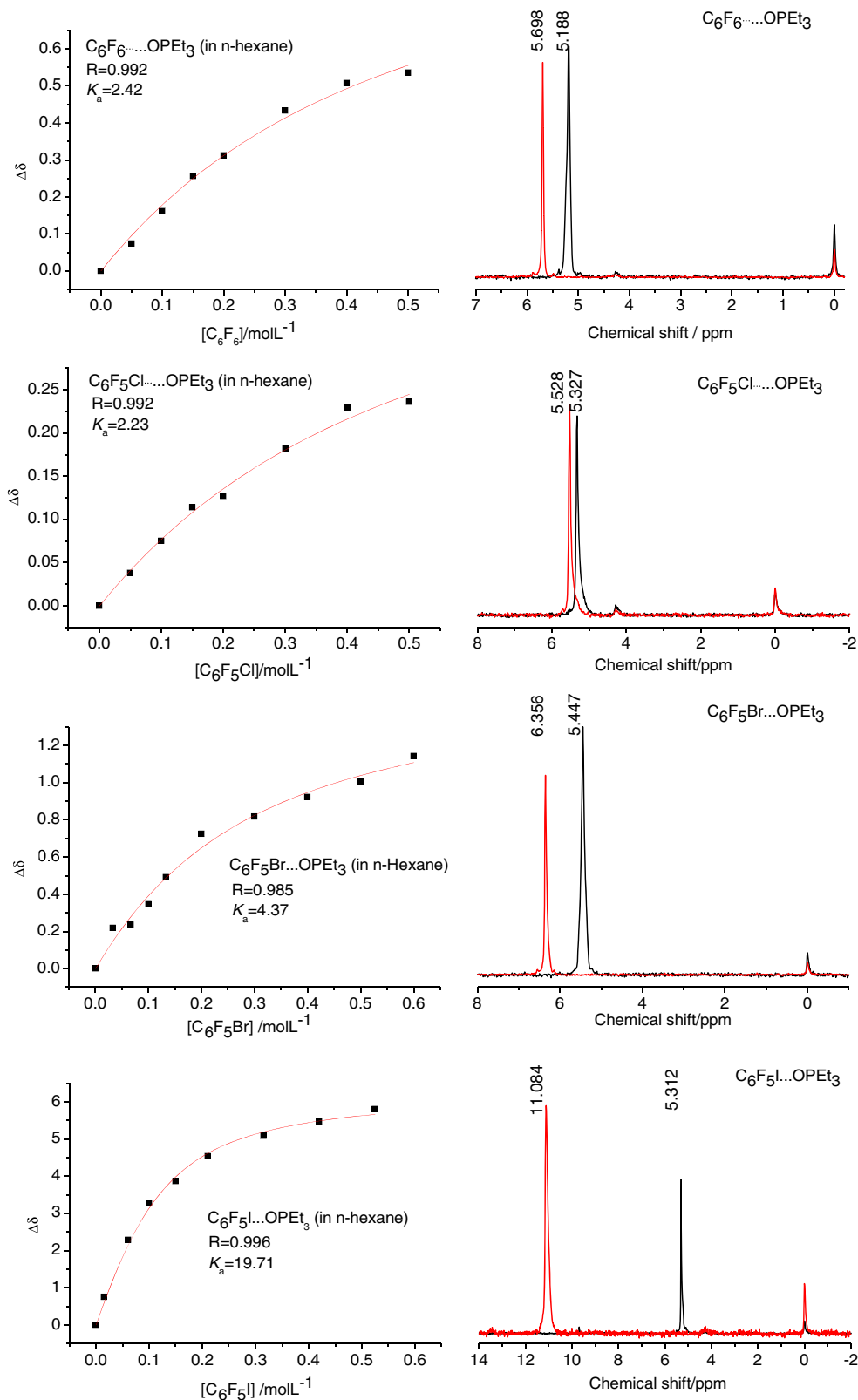
Above optimized structural data show the possibility of  $\sigma$ -hole bonding and  $\pi$ -hole bonding complexes, which agrees with the conclusion from analyzing surface electrostatic potentials. However, for C<sub>6</sub>F<sub>5</sub>Cl, C<sub>6</sub>F<sub>5</sub>Br and C<sub>6</sub>F<sub>5</sub>I, both  $\sigma$ -hole and  $\pi$ -hole bonds are possible. So, it is assumed that  $\sigma$ -hole bond and  $\pi$ -hole bond could take place simultaneously to form the trimer complex (*vide* Fig. 2). The optimized structural parameters of trimer complexes were listed in Table 1.

**Table 2** Interaction energies (in kcal mol<sup>-1</sup>) of  $\sigma$ -hole and  $\pi$ -hole bonding complexes in solution

Complexes		$\Delta E$		$\Delta E_{coop}$
		$\pi$ -hole bond	$\sigma$ -hole bond	
C <sub>6</sub> F <sub>6</sub> $\cdots$ O=PMe <sub>3</sub>	dimer	-7.29	/	/
C <sub>6</sub> F <sub>5</sub> Cl $\cdots$ O=PMe <sub>3</sub>	dimer	-7.24	-3.37	2.23
C <sub>6</sub> F <sub>5</sub> Cl $\cdots$ (O=PMe <sub>3</sub> ) <sub>2</sub>	trimer	-6.09	-2.29	/
C <sub>6</sub> F <sub>5</sub> Br $\cdots$ O=PMe <sub>3</sub>	dimer	-7.19	-5.07	1.18
C <sub>6</sub> F <sub>5</sub> Br $\cdots$ (O=PMe <sub>3</sub> ) <sub>2</sub>	trimer	-6.63	-4.45	/
C <sub>6</sub> F <sub>5</sub> I $\cdots$ O=PMe <sub>3</sub>	dimer	-6.79	-8.25	2.53
C <sub>6</sub> F <sub>5</sub> I $\cdots$ (O=PMe <sub>3</sub> ) <sub>2</sub>	trimer	-5.53	-6.98	/

Compared with practical dimer, the bond lengths of  $\sigma$ -hole bond and  $\pi$ -hole bond in trimer are longer. In terms of bond length change, it implies that two interactions are competitive. One can decline or destruct another one.

**Fig. 3** Plot of  $|\Delta\delta|$  (ppm) against titrated  $[C_6F_5X]$  ( $\text{mol L}^{-1}$ ) under fixed  $[Et_3P=O]$   $0.1 \text{ mol L}^{-1}$  (left) and  $^3P$  NMR of  $Et_3PO$  before and after adding  $C_6F_5X$  (right)



## Interaction energies and cooperative energies

Interaction energy is another important parameter to characterize the bonding strength. Herein, the large basis sets have to be used to eliminate the basic set superposition error (BSSE) because the counterpoise method could not be used to correct the BSSE in calculating interaction in solution using SMD model. The interaction energies calculated by  $\omega$ B97X-D with mixed base sets 6-311++G\*\*/LANL2DZdp are listed in Table 2.

In terms of  $\pi$ -hole bond, interaction energy of  $\pi$ -hole bonding complex decreases gradually as decrease of electron-withdrawing ability from F, Cl, Br to I. But the change range in energy is not large. For example, for  $C_6F_6$ , the  $\pi$ -hole bonding energy is  $-7.29 \text{ kcal mol}^{-1}$ , while  $-6.79 \text{ kcal mol}^{-1}$  for  $C_6F_5I$ , only change  $0.5 \text{ kcal mol}^{-1}$ . The results should be a sequency of little change in surface electrostatic potential of  $\pi$ -hole from  $C_6F_6$ ,  $C_6F_5Cl$ ,  $C_6F_5Br$  and  $C_6F_5I$  as mentioned above. So, the distance between O to the center-o shows small change range,  $0.051 \text{ \AA}$ .

In terms of  $\sigma$ -hole bond, i.e., halogen bond, it can be seen from Table 1 that both the halogen bonding energy and length of O to X (X=Cl, Br, I) in dimer show larger change range, for example,  $-3.37$ ,  $-5.07$  and  $-8.25 \text{ kcal mol}^{-1}$  for  $C_6F_5Cl \cdots O=P$ ,  $C_6F_5Br \cdots O=P$  and  $C_6F_5I \cdots O=P$ , respectively, the change range in energy is  $4.88 \text{ kcal mol}^{-1}$ . The change range of distance between O to the  $\sigma$ -hole center-o is  $0.081 \text{ \AA}$  from  $C_6F_5Cl$  to  $C_6F_5I$ . So, the change in geometer parameters reflects the change of surface electrostatic potential of  $\sigma$ -hole and ability of halogen to form halogen bond.

For  $C_6F_6$ , the  $\pi$ -hole bonding to electron-rich site, halide ion, lone electron pair or  $\pi$ -system etc., is sole specific interaction pattern. However, for  $C_6F_5X$ , both  $\pi$ -hole and  $\sigma$ -hole bonding patterns to electron-negative site are possible. The question is that  $\pi$ -hole and  $\sigma$ -hole bonds are cooperative or competitive? And which one is predominant if competitive? Firstly, the analysis is carried out by comparing the difference of surface electrostatic potential at  $\pi$ -hole center-o or  $\sigma$ -hole and interaction energy in dimer. For  $C_6F_5Cl$ , the difference in electrostatic potential of  $\pi$ -hole and  $\sigma$ -hole is small ( $21.4$  v.s.  $19.3 \text{ kcal mol}^{-1}$ ), but the difference in interaction energies of  $\pi$ -hole bond and  $\sigma$ -hole bond is larger ( $7.24$  v.s.  $3.37 \text{ kcal mol}^{-1}$ ). So,  $\pi$ -hole bond of  $C_6F_5Cl$  to  $O=P$  is predominant. For  $C_6F_5Br$ , the electrostatic potential at  $\sigma$ -hole is higher than that at  $\pi$ -hole,  $27.5$  vs  $20.6 \text{ kcal mol}^{-1}$ . It

seems the halogen bond of  $C_6F_5Br$  to  $O=P$  is main. However, the interaction energy of  $\pi$ -hole  $\cdots O=P$  bond is  $-7.19 \text{ kcal mol}^{-1}$ , being stronger than  $-5.07 \text{ kcal mol}^{-1}$  of  $\sigma$ -hole  $\cdots O=P$  bond. It is believed that the actual interaction energy of halogen bond of  $C_6F_5Br$  to  $O=P$  should be greater, leading to the two bonds coexisting competitively. For  $C_6F_5I$ , in terms of electrostatic potential and interaction energy, halogen bond  $C_6F_5I \cdots O=P$  is preponderant.

Secondly, the calculation on individual interaction energies of  $\sigma$ -hole bond and  $\pi$ -hole bond as well as the cooperative energy in trimer (*vide* Fig. 2) may provide useful information on the relationship of  $\sigma$ -hole bond and  $\pi$ -hole bond. Table 2 shows that the interaction energies of  $\sigma$ -hole bond and  $\pi$ -hole bond in trimer are all smaller than that in dimer, meaning the occurrence of one could weaken or destruct another one. That is, the two are competitive in present systems. Moreover, it is noticed that the  $\pi$ -hole bond  $C_6F_5Br \cdots O=PMe_3$  in trimer is stronger than  $C_6F_5Cl$  and  $C_6F_5I$ ,  $-6.63 \text{ kcal mol}^{-1}$  for  $C_6F_5Br \cdots O=PMe_3$ ,  $-6.09 \text{ kcal mol}^{-1}$  for  $C_6F_5Cl \cdots O=PMe_3$  and  $-5.53 \text{ kcal mol}^{-1}$  for  $C_6F_5I \cdots O=PMe_3$ . In all cases, the positive cooperative energy in trimer,  $\Delta E_{\text{coop}}$ ,  $2.23 \text{ kcal mol}^{-1}$  for  $C_6F_5Cl$ ,  $1.18 \text{ kcal mol}^{-1}$  for  $C_6F_5Br$  and  $2.53 \text{ kcal mol}^{-1}$  for  $C_6F_5I$ , should indicate the competition of  $\sigma$ -hole bond and  $\pi$ -hole bond. The declining magnitude of the two bonds or cooperative energy for  $C_6F_5Br$  is smallest. It may imply for  $C_6F_5Br$ , the competition of the two bonds is weaker, they might coexist in solution. It is consistent with the experimental results as mentioned later.

The determination of bonding constants by  $^{31}\text{P}$  NMR

NMR is one of the important methods to investigate the intermolecular interaction in solution which can be used to determine the association or bonding constants of supramolecular complexes [4, 30, 31, 42–45]. The change of oxygen electron density as halopentafluorobenzenes interact with triethylphosphine oxide can affect the  $^{31}\text{P}$  NMR chemical shift. Here the interaction between halopentafluorobenzenes and triethylphosphine oxide is studied and bonding constants are determined by  $^{31}\text{P}$  NMR. Compared with previous reports [4, 30, 42, 43], the difference is that here n-hexane is used as inert solvent to eliminate the influence of different solvation of monomer and complex on the  $^{31}\text{P}$  chemical shift.

The chemical shifts and the largest value of  $^{31}\text{P}$  NMR in n-hexane as the titration of halopentafluorobenzenes are shown

**Table 3** The experimental  $^{31}\text{P}$  NMR data for  $\text{Et}_3\text{PO} \cdots \text{C}_6\text{F}_5\text{X}$ : binding constants, the maximum  $^{31}\text{P}$ NMR chemical shift (in ppm) and correlation coefficient

	$C_6F_6 \cdots OPEt_3$	$C_6F_5Cl \cdots OPEt_3$	$C_6F_5Br \cdots OPEt_3$	$C_6F_5I \cdots OPEt_3$
$K_a/M^{-1}$	2.42	2.23	4.37	19.7
$\Delta\delta_{\text{max}}/\text{ppm}$	1.068	0.488	1.586	6.403
$R^2$	0.992	0.992	0.985	0.996

in Fig. 3. It can be seen that chemical shifts of  $^{31}\text{P}$  NMR shift down field as the titration of halopentafluorobenzenes and the shift is the largest for  $\text{C}_6\text{F}_5\text{I}$  and smallest for  $\text{C}_6\text{F}_5\text{Cl}$ . The plots of observed change  $\Delta\delta$  in chemical shift to the concentration of  $\text{C}_6\text{F}_5\text{X}$  can be fitted by Eqs. (1) and (2) by which the  $K_a$  is obtained, as listed in Table 3.

The bonding constant of the complex between  $\text{C}_6\text{F}_6$  and triethylphosphine oxide is  $2.42\text{ M}^{-1}$ , while it is  $19.7\text{ M}^{-1}$  between  $\text{C}_6\text{F}_5\text{I}$  and triethylphosphine oxide. Also the largest values of  $^{31}\text{P}$  NMR chemical shift as  $\text{C}_6\text{F}_6$  or  $\text{C}_6\text{F}_5\text{X}$  if enough was added are different,  $1.068$  vs  $6.403$  ppm, respectively. So large difference indicates the interaction form should be different for  $\text{C}_6\text{F}_6$  and  $\text{C}_6\text{F}_5\text{I}$  with same acceptor. From the prediction based on surface electrostatic potentials,  $\text{C}_6\text{F}_6$  produces single  $\pi$ -hole bond with triethylphosphine oxide, and if  $\text{C}_6\text{F}_5\text{I}$  also produce the  $\pi$ -hole bond, the bonding constants of the complex should be close to or smaller than that of  $\text{C}_6\text{F}_6$  because their  $\pi$ -hole potentials display no remarkable difference. The fact shows  $\text{C}_6\text{F}_5\text{I}$  produces the  $\sigma$ -hole bond instead of  $\pi$ -hole bond with triethylphosphine oxide. The results support the conclusions mentioned above  $\text{C}_6\text{F}_5\text{I}$  produces the  $\sigma$ -hole bond and its strength is higher than  $\pi$ -hole bond of itself or  $\text{C}_6\text{F}_6$ ,  $\text{C}_6\text{F}_5\text{I}\cdots\text{O}=\text{P}$ ,  $-8.25$  ( $\sigma$ -hole bond) vs  $\text{C}_6\text{F}_5\text{I}\cdots\text{O}=\text{P}$   $-6.79$  ( $\pi$ -hole bond)  $\text{kcal mol}^{-1}$  or  $\text{C}_6\text{F}_6\cdots\text{O}=\text{P}$   $-7.29$   $\text{kcal mol}^{-1}$ , see Table 2.

The bonding constant and the largest change  $\Delta\delta_{\text{max}}$  of  $^{31}\text{P}$  by interaction with  $\text{O}=\text{PET}_3$  for  $\text{C}_6\text{F}_5\text{Cl}$  are all close to  $\text{C}_6\text{F}_6$ . Combining the calculation, it is concluded that  $\text{C}_6\text{F}_5\text{Cl}$  also produces the  $\pi$ -hole bond with  $\text{O}=\text{P}$  the same as  $\text{C}_6\text{F}_6$ . For  $\text{C}_6\text{F}_5\text{Br}$ , there are comparative  $\sigma$ -hole and  $\pi$ -hole bonding ability, the bonding constant of  $4.37\text{ M}^{-1}$  is larger than  $2.23\text{ M}^{-1}$  of  $\text{C}_6\text{F}_5\text{Cl}$ , but much lower than  $19.7\text{ M}^{-1}$  of  $\text{C}_6\text{F}_5\text{I}$ . So, it should indicate the  $\sigma$ -hole and  $\pi$ -hole bond coexist in solution competitively.

## Conclusions

The perfluorobenzene  $\text{C}_6\text{F}_6$  and chloropentafluorobenzene  $\text{C}_6\text{F}_5\text{Cl}$  interact with triethylphosphine oxide by  $\pi$ -hole bonding pattern, while  $\text{C}_6\text{F}_5\text{I}$  by halogen/ $\sigma$ -hole bond. For  $\text{C}_6\text{F}_5\text{Br}$ , two interactions are comparative and should coexist competitively. The calculated interaction energies of  $\sigma$ -hole and  $\pi$ -hole bonding complexes are consistent with the changing tendency of bonding constants measured by  $^{31}\text{P}$  NMR. The electrostatic interaction, polarization and dispersion contribute to the halogen/ $\sigma$ -hole bond, while  $\pi$ -hole bond is mainly driven by electrostatic interaction. The investigation should be significant in research on interaction involved in aromatic systems, especially the systems with  $\pi$ -hole, also in understanding the stability of biological structure and anion recognition, and so on.

**Acknowledgments** Financial supports from the National Natural Science Foundation of China (No.90922023), Ph. D foundation program of Ministry of Education (No.20110003110011) are gratefully acknowledged. We also appreciate very much the reviewers and editor's valuable suggestions and advice on this paper.

## References

1. Metrangolo P, Resnati G (2008) *Science* 321:918–919
2. Zhao XR, Shen QJ, Jin WJ (2013) *Chem Phys Lett* 566:60–66
3. Metrangolo P, Neukirch H, Pilati T, Resnati G (2005) *Acc Chem Res* 38:386–395
4. Gao K, Goroff NS (2000) *J Am Chem Soc* 122:9320–9321
5. Parisini E, Metrangolo P, Pilati T, Resnati G, Terraneo G (2011) *Chem Soc Rev* 40:2267–2268
6. Zhao XR, Wu YJ, Han J, Shen QJ, Jin WJ (2013) *J Mol Model* 19: 299–304
7. Clark T, Hennemann M, Murray JS, Politzer P (2007) *J Mol Model* 13:291–296
8. Murray JS, Lane P, Politzer P (2009) *J Mol Model* 15:723–729
9. Hohenstein EG, Duan J, Sherrill CD (2011) *J Am Chem Soc* 133: 13244–13247
10. Tsuzuki S, Honda K, Uchimaru T, Mikami M, Tanabe K (2002) *J Am Chem Soc* 124:104–112
11. Sinnokrot MO, Sherrill CD (2006) *J Phys Chem A* 110:10656–10668
12. Chandrasekaran V, Biennier L, Arunan E, Talbi D, Georges R (2011) *J Phys Chem A* 115:11263–11268
13. Wheeler SE (2011) *J Am Chem Soc* 133:10262–10274
14. Wheeler SE, Houk KN (2008) *J Am Chem Soc* 130:10854–10855
15. Hobza P, Selzle HL, Schlag EW (1996) *J Phys Chem* 100:18790–18794
16. Salonen LM, Ellemann M, Diederich F (2011) *Angew Chem Int Ed* 50:4808–4842
17. Mascal M, Armstrong A, Bartberger MD (2002) *J Am Chem Soc* 124:6274–6276
18. Quiñero D, Garau C, Rotger C, Frontera A, Ballester P, Costa A, Deyà PM (2002) *Angew Chem Int Ed* 41:3389–3392
19. Mooibroek TJ, Gamez P, Reedijk J (2008) *CrystEngComm* 10:1501–1515
20. Ma JC, Dougherty DA (1997) *Chem Rev* 97:1303–1324
21. Schottel BL, Chifotides HT, Dunbar KR (2008) *Chem Soc Rev* 37: 68–83
22. Berryman OB, Bryantsev VS, Stay DP, Johnson DW, Hay BP (2007) *J Am Chem Soc* 129:48–58
23. Wheeler SE, Houk KN (2010) *J Phys Chem A* 114:8658–8664
24. Pang X, Wang H, Zhao XR, Jin WJ (2013) *CrystEngComm* 15: 2722–2730
25. Politzer P, Murray JS, Clark T (2010) *Phys Chem Chem Phys* 12: 7748–7757
26. Politzer P, Murray JS, Clark T (2013) *Phys Chem Chem Phys* 15: 11178–11189
27. Murray JS, Lane P, Clark T, Riley KE, Politzer P (2012) *J Mol Model* 18:541–548
28. Politzer P, Riley KE, Bulat FA, Murray JS (2012) *Comp Theor Chem* 998:2–8
29. Politzer P, Murray JS (2013) *ChemPhysChem* 14:278–294
30. Ma N, Zhang Y, Ji BM (2012) *ChemPhysChem* 13:1411–1414
31. Zhang Y, Ji BM, Tian AM, Wang WZ (2012) *J Chem Phys* 136: 141101-1–141101-4
32. Frisch MJ, Trucks GW, Schlegel HB, Scuseria GE, Robb MA, Cheeseman JR, Scalmani G, Barone V, Mennucci B, Petersson GA, Nakatsuji H, Caricato M, Li X, Hratchian HP, Izmaylov AF, Bloino J, Zheng G, Sonnenberg JL, Hada M, Ehara M, Toyota K, Fukuda R,

- Hasegawa J, Ishida M, Nakajima T, Honda Y, Kitao O, Nakai H, Vreven T, Montgomery JA Jr, Peralta JE, Ogliaro F, Bearpark M, Heyd JJ, Brothers E, Kudin KN, Staroverov VN, Kobayashi R, Normand J, Raghavachari K, Rendell A, Burant JC, Iyengar SS, Tomasi J, Cossi M, Rega N, Millam JM, Klene M, Knox JE, Cross JB, Bakken V, Adamo C, Jaramillo J, Gomperts R, Stratmann RE, Yazyev O, Austin AJ, Cammi R, Pomelli C, Ochterski JW, Martin RL, Morokuma K, Zakrzewski VG, Voth GA, Salvador P, Dannenberg JJ, Dapprich S, Daniels AD, Farkas Ö, Foresman JB, Ortiz JV, Cioslowski J, Fox DJ (2009) Gaussian 09, Revision A.02. Gaussian, Inc, Wallingford
33. Chai JD, Head-Gordon M (2008) *Phys Chem Chem Phys* 10:6615–6620
34. Chai JD, Head-Gordon M (2008) *J Chem Phys* 128:084106-1–084106-15
35. Marenich AV, Cramer CJ, Truhlar DG (2009) *J Phys Chem B* 113: 6378–6396
36. Hughes MP, Shang M, Smith BD (1996) *J Org Chem* 61:4510–4511
37. Gao HY, Shen QJ, Zhao XR, Yan XQ, Pang X, Jin WJ (2012) *J Mater Chem* 22:5336–5343
38. Ji BM, Wang WZ, Deng DS, Zhang Y (2011) *Cryst Growth Des* 11: 3622–3628
39. Shen QJ, Wei HQ, Zou WS, Sun HL, Jin WJ (2012) *CrystEngComm* 14:1010–1015
40. Shen QJ, Pang X, Zhao XR, Gao HY, Sun HL, Jin WJ (2012) *CrystEngComm* 14:5027–5034
41. Riley KE, Murray JS, Fanfrlík J, Řezáč J, Solá RJ, Concha MC, Ramos FM, Politzer P (2011) *J Mol Model* 17:3309–3318
42. Rege PD, Malkina OL, Goroff NS (2002) *J Am Chem Soc* 124:370–371
43. Moss WN, Goroff NS (2005) *J Org Chem* 70:802–808
44. Morishima I, Endo K, Yonezawa T (1971) *J Am Chem Soc* 93:2048–2050
45. Hauchecorne D, van der Veken BJ, Herrebout WA, Hansen PEA (2011) *Chem Phys* 381:5–10